Article

Revealing the Cell Entry Dynamic Mechanism of Single Rabies Virus Particle

LI Siying[1#], PAN Yangang[2#], TENG Honggang[2], SHAN Yuping[1✉], YANG Guocheng[1] and WANG Hongda[2✉]

Received March 2, 2022
Accepted March 31, 2022

The rabies virus is a neurotropic virus that causes fatal diseases in humans and animals. Although studying the interactions between a single rabies virus and the cell membrane is necessary for understanding the pathogenesis, the internalization dynamic mechanism of single rabies virus in living cells remains largely elusive. Here, we utilized a novel force tracing technique based on atomic force microscopy(AFM) to record the process of single viral entry into host cell. We revealed that the force of the rabies virus internalization distributed at (65±25) pN, and the time was identified by two peaks with spacings of (237.2±59.1) and (790.3±134.4) ms with the corresponding speed of 0.12 and 0.04 μm/s, respectively. Our results provide insight into the effects of viral shape during the endocytosis process. This report will be meaningful for understanding the dynamic mechanism of rabies virus early infection.

Keywords Rabies virus; Entering host cell; Dynamic mechanism; Atomic force microscopy(AFM); Force tracing

1 Introduction

Rabies virus(RV) is an enveloped and negative single-strand RNA virus, which belongs to the Lyssavirus genus of the Rhabdovindae family[1−3]. Infection usually begins in muscle tissue following a bite from an infected animal[4]. The RNA genome of RV consists of five genes encoding viral proteins: nucleoprotein, phosphoprotein, matrix protein, glycoprotein, and, viral RNA polymerase[5]. The bullet-shaped particles were found to differ in diameter(45—100 nm) and length(100—430 nm), and the viral determinant for RV infection is the glycoprotein spikes on the exterior of RV[6,7]. The glycoprotein spikes must bind to cellular membrane receptors for mediating rabies viral entry. After G spikes interacting with cell membrane receptors, the virus enters into living cell by endocytosis. Subsequently, the virus takes advantage of the acidic environment of the endosome to release five proteins and single-strand RNA in the cytoplasm[7,8].

RV is a dangerous pathogen that drives deadly diseases in humans and animals[4]. Although the entry pathway and viral life cycle have been researched by electron micrographs[9,10] and fluorescence microscopy[11,12], little is known about the internalization dynamic process for RV particles entering cell. However, understanding how bullet-like shaped RV particles enter cells is important for explaining RV early infection. Virus entering cell is a dynamic process, and transporting force, duration, and average speed are key points during the cellular uptake. The most prominent advantage of the force tracing technique based on atomic force microscopy(AFM) is the high temporal-spatial resolution, and it has been considered as a powerful tool for studying the cell membrane function at single molecue/particle level under physiological conditions, especially tracking the transport dynamic process of substance from extracellular to intracellular[13−15]. The force tracing technique has been used to sucessfully monitor the dynamic process of single Ebola virus particle invagination behavior[13]. Herein, we used the AFM-based force tracing to capture the ultrafast process of single RV particles invagination under native environments and explore the dynamic mechanism of the cellular uptake of bullet shape RV particle. The results will provide a new perspective on the cells infected by a bullet shape RV at the single-molecule level.

2 Experimental

2.1 Cell Culture

Vero cells were obtained from Shanghai Institutes of Biological Sciences(Shanghai, China). The cells were cultured in a Dulbecco's modified Eagle's medium(DMEM) containing 10% fetal bovine serum, 100 U/mL penicillin, and 100 μg/mL streptomycin at 37 °C with 5% CO_2. Usually, the cells need to be cultured for 24 or 48 h to achieve 75% confluence on the glass slide. Before force tracing test, the cells were washed with PBS(phosphate buffer solution, 137 mmol/L NaCl, 2 mmol/L KCl, 8 mmol/L Na_2HPO_4, and 1.5 mmol/L KH_2PO_4, pH 7.4) three times and serum-free medium once in sequence to remove cell debris.

✉ WANG Hongda
hdwang@ciac.ac.cn
✉ SHAN Yuping
shanyp@ciac.ac.cn
# These authors contributed equally to this work.
1. School of Chemistry and Life Science, Advanced Institute of Materials Science, Changchun University of Technology, Changchun 130012, P. R. China;
2. State Key Laboratory of Electroanalytical Chemistry, Changchun Institute of Applied Chemistry, Chinese Academy of Sciences, Changchun 130022, P. R. China

https://doi.org/10.1007/s40242-022-2069-y

2.2 Tip Chemistry

The AFM tips(Microlever, Veeco, Santa Barbara, CA) were cleaned in a UV cleaner and vapor treated with APTES. Subsequently, PEG-crosslinker(benzaldehyde-PEG$_{76}$-NHS, FW: 3962, SensoPath Technologies, Bozeman, MT) was conjugated in triethylamine and trichloromethane as described[16]. After drying with argon, the AFM tips were immersed in a mixture of RV particles(100 μL) in PBS and 1 mol/L $NaCNBH_3$(4 μL). After functionalization for 1 h, 1 mol/L ethanomine(10 μL) was added to the solution in order to passivate the unreacted aldehyde groups. Then the AFM tips were washed with PBS three times and stored at 4 °C.

2.3 Force Tracing Measurements

Force tracing curves were acquired based on AFM 5500 (Agilent Technologies, Chandler, AZ) in DMEM at 37 °C controlled by a temperature controller 325(Agilent Technologies, Chandler, AZ). The small shifts of the cantilever-deflection signal were collected by a 16 bit DA/AD card(PCI-6361e, National Instruments). The blocking experiments were performed by the addition of cytochalasin B(the final concentration is 1 μg/mL), chlorpromazine(the final concentration is 10 μg/mL), and filipin(the final concentration is 10 μg/mL) to the cell culture medium for 30 min, respectively. Thousands of force tracing curves were recorded at different positions on the cells. The deflection sensitivity and the spring constant of AFM tip were determined as previous report[17]. The data were collected with the low-pass filter of 100 Hz to get rid of high frequency noise from the electronics and environment.

2.4 Cell and RV Particle Labeling

To label cells with the lipophilic dye Dio, the cells were incubated with Dio dissolved in dimethyl sulfoxide(DMSO, 2 μL, 1 mg/mL) at room temperature for 30 min. To label the RV particles with amine-reactive Cy5(OPE TECH), RV particle stock was incubated with Cy5-NHS in PBS at room temperature for 1 h and the unincorporated dye was removed by centrifugation three times at 16000 r/min and 4 °C for 50 min(TGL-20M).

3 Results and Discussion

In our study, we selected Vero cell line as model to study the RV particle internalization due to the relative flat profile of Vero cells, which is helpful for obtaining more clear force-time signal.

3.1 RV Particles Functionalized AFM Tip for Force Tracing Test

We first tested RV-infected Vero cells with fluorescence imaging to confirm that the used RV particles(*ca*. 60 nm) could enter living cells. After the co-incubation of Vero cells with RV particles at 37 °C for 2 h, the cells were imaged by the real-time confocal microscopy, and the fluorescence image is shown in Fig.1(A). Then we used the force tracing to capture the ultrafast process of endocytosis of single RV particles by Vero cells. Fig.1(B) shows the setup principle of force tracing technique with the help of a CCD camera(Fig.S1, see the Electronic Supplementary Material of this paper). RV particles functionalized AFM tip is located above cell membrane, and a laser beam strikes the AFM tip cantilever and is reflected by a photodetector to detect the deflection of the AFM tip cantilever. The deflection variation with time can be recoreded and the force-time curves were obtained. For performing force tracing measurement, we firstly determine the contact point by performing traditional single molecule force spectroscopy (Fig.S2, see the Electronic Supplementary Material of this paper), and then the RV particles functionalized AFM tip is

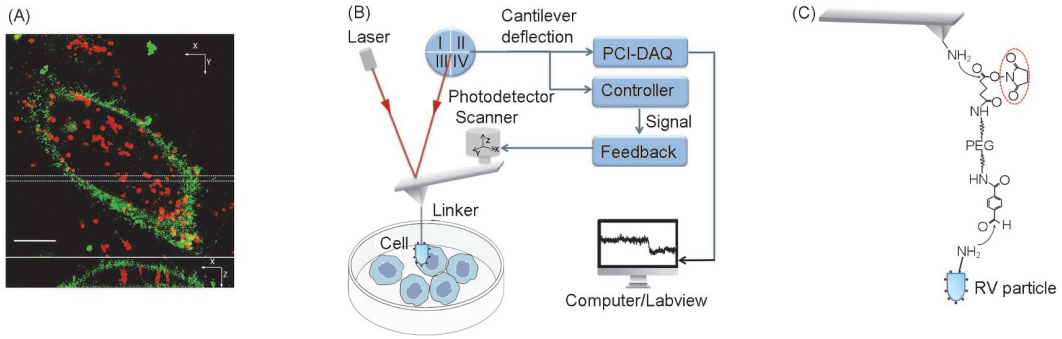

Fig.1 Principle and process of force tracing technique

(A)Three-dimensional confocal images of Vero cell infected with RV particles(red). To construct the *X-Z* image plane, successive z-stacks spaced by 200 nm were recorded. The *X-Y* image plane is located at the upper surface of the cell. The *X-Z* image plane is located between the dashed lines. Scale bar is 10 μm; (B) the schematic setup of force tracing based on AFM and PCI-DAQ; (C) the scheme of a functionalized AFM tip. The RV particles were covalently coupled to AFM tip *via* a heterobifunctional PEG linker.

https://doi.org/10.1007/s40242-022-2069-y

moved to the contact point by adjusting the AFM feedback system[the proportional-integral(PI) control system, I and P are 0.001]. Subsequently, we turn off the feedback system and the AFM tip is tethered with the RV particles slightly contacting the cell membrane. Once RV particle is endocytosed, the AFM tip cantilever tethered RV particles will bend downwards, and the PCI-DAQ card will record the internalization force and duration. The 20 kHz sampling rate is selected that can easily monitor the fast process down to 1 μs and is suitable for recording the ultrafast process of virus endocytosed by living cells. RV particles were covalently conjugated onto the AFM tip *via* heterobifunctional PEG(benzaldehyde-PEG$_{76}$-NHS) linker for recording the process of viral invagination by force tracing technique, and the length of the PEG linker is approximately 33 nm, which is suitable for capturing the ultrafast process of the RV particles endocytosis(cell membrane thickness is about 20 nm)[18]. The NHS ester terminus end of the PEG linker is immobilized on the aminated AFM tip, and the benzaldehyde moiety at the other end reacts with the amino group of the RV particle. The tip chemistry is illustrated in Fig.1(C).

3.2 Force Tracing Test

Usually, we locate the RV particles modified AFM tip cantilver on one cell membrane and record the deflection-time curve(which could be converted into force-time curve) for 20 min, and the data are divided into several files according to time(*ca.* 12 s/file). After *ca.* 20 min detecting, the AFM tip will be retracted and changed to another region, and about 200 curves are collected from one cell. Then 2000—3000 force curves are obtained from 10—15 cells at different positions. There are two typical types of force-time signals recording RV particles invagination, denoted as Fig.2(A) and (B). The time and force of RV particles invaginating into cell membrane can be measured through the force tracing curves directly. The force tracing signal begins from the left to the right. Initially, the left side of the curve is flat because the RV particles are just located on the cell membrane. As the RV particles on the AFM tip internalize into cell membrane, the PEG linker will be stretched and further induces AFM tip cantilever bending downwards, and a force-time signal can be detected(red arrows). The *X*-axis in the typical force tracing curve shows time, and the distance between the start point and the end point of the *X*-axis represents the duration for the completion of a single RV particle internalization. The *Y*-axis in the typical force tracing curve represents the force converted from the AFM tip cantilever deflection, and the distance between the start point and the end point of *Y*-axis represents the force for the completion of internalization of a single RV particle. Then the endocytosis force and the force from AFM cantilever reach equilibrium, and the force tracing curve returns to flat(right side). The force of the RV particles internalization is at a distribution of about (65±25) pN(mean±stand deviation), as shown in Fig.2(C). From the force distribution histogram, only one peak of force values was obtained[Fig.2(C)]. Interestingly, by analyzing the force tracing curves, the time was identified by two peaks with spacings of (237.2.1±59.1) and (790.3±134.4) ms, as shown in Fig.2(D). It is reported that a work investigated by computer simulation found that the shape and the initial orientation of the particle are crucial to the nature of the interaction between the particle and lipid bilayer[19]. Recently, Shan *et al.*[13] found the filamentous Ebola virus might enter cells in both horizontal and vertical modes. Here, we speculated that the RV particles on the tip interacted with cell membrane by different modes: (i) the RV particles interact with

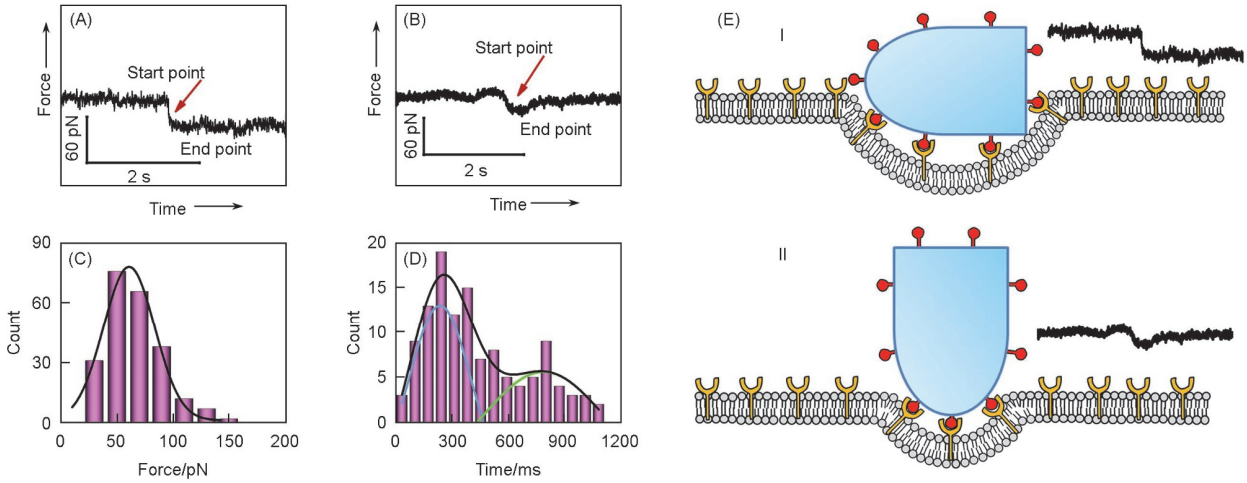

Fig.2 Two types of force tracing curves of RV particles endocytosis

(A, B) Two types of typical force tracing curves showing the RV particles enter living cells; (C) distribution of force for RV particles entering living cell; (D) time distribution of RV particles during internalization. Blue and green curves represent individual Gaussian fits, and black curve is automated multipeak fitting. n≈200; (E) schematic showing the interaction between RV particles and cell membrane with different modes.

https://doi.org/10.1007/s40242-022-2069-y

cell membrane horizontally[Fig.2(E), I]; (ii) the RV particles interact with cell membrane vertically or at a small angle [Fig.2(E), II]. This suggests that the interaction mode between RV particles and cell membrane could affect the viral invagination time. Clean AFM tip was also used to perform the force tracing test on the living cell under the same conditions and few force-time signals are observed, as illustrated in Fig.S3(see the Electronic Supplementary Material of this paper). Based on these results, we inferred that the force-time signal in force tracing curve observed was attributed to the viral entry.

3.3 Calculations of Displacement

To further study the ultrafast process of the RV particles entering into cells, we measured the displacement D during the internalization. Schematic diagram of displacement calculation is shown in Fig.3(A), which can be expressed as Equation (1):

$$D=d+x \tag{1}$$

where d is the bending distance of the AFM tip cantilever, and x is the stretching length of the PEG linker. The d can be calculated from Hooke's law[Equation (2)]:

$$d=F/k \tag{2}$$

where F is the force measured in force tracing curves, and k is the spring constant of the AFM tip cantilever. The x can be calculated from the worm like chain model[Equation (3)][20]:

$$\frac{FL_p}{K_BT}=\frac{1}{4}\left(1-\frac{x}{L_0}+\frac{F}{K_0}\right)^{-2}-\frac{1}{4}+\frac{x}{L_0}-\frac{F}{K_0} \tag{3}$$

where T is the Kelvin temperature, K_B represents the Boltzmann constant, L_P represents the persistence length set to (3.8±0.02) Å(1 Å =0.1 nm), and K_0 is the enthalpic correction set to (1561±33) pN as suggested[20]. The contour length L_0 for 76—77 mers of PEG is 326 Å in consideration of that per PEG length is 4.2 Å and the termini is 5.25 Å. Fig.3(B) shows the displacement of RV particles during internalization according to the force that caused by the RV particles entering cells, and the displacement ranges from 21 nm to 34 nm with a mean value of 28 nm, which can also be attributed to the two modes of RV particles entering cell. In our study, the RV particle displacement is only related to the force we detected, which means that the RV particles invagination speed is different [Fig.3(C)]. The mean speeds during the endocytosis process (D/t) are 0.12 and 0.04 μm/s.

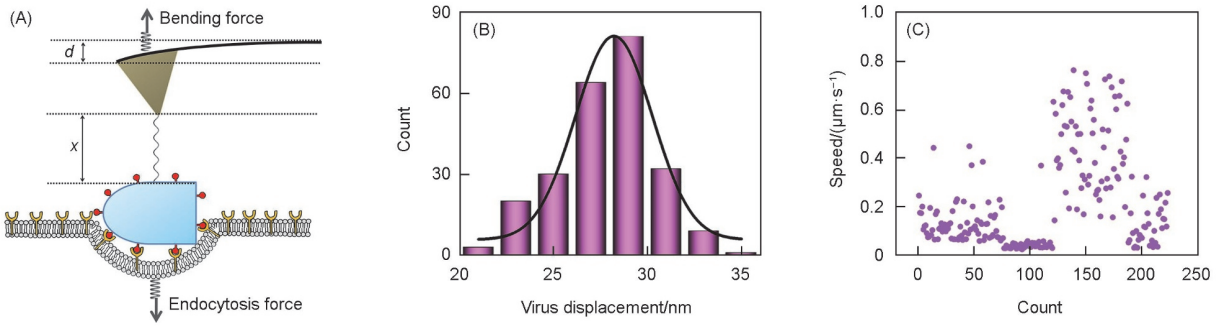

Fig.3 Displacement of RV particles during internalization according to the force tracing measuring

(A) Schematic diagram of displacement calculation for RV particles during internalization; (B) RV particle displacement distribution caused by cellular uptake; (C) scatter diagram of speed during RV particles entering cell.

3.4 Mechanism of RV Cell Entry

The critical step in all viral infection involves the penetration of the viral particles into the cytosol. For this reason, viruses make use of the endocytic membrane trafficking to enter the host cell[21]. Endocytosis is an important mechanism for cells to ingest extracellular components by modulating the plasma membrane[22], and most viruses use receptor-mediated endocytosis to enter their host cells, such as severe acute respiratory syndrome coronavirus 2(SARS-CoV-2)[23,24]. The endocytic pathway includes clathrin-mediated endocytosis[25], caveolae-meidiated endocytosis[26], macropinocytosis[27] and so on. Clathrin-mediated endocytosis and caveolae-mediated endocytosis are two main pathways[28,29]. In order to further investigate the pathway of RV particles internalization, a series of blocking experiments was performed. Clathrin-mediated endocytosis inhibitor chlorpromazine(CPZ, a final concentration of 10 μg/mL), and caveolae-dependent endocytosis inhibitor filipin(a final concentration of 10 μg/mL) were used to co-incubate with Vero cells, respectively. As shown in Fig.4(A), the probability of observing force-time signal decreases to 2.2% and 5.12%, respectively(control: 9.85%) after injecting cytochalasin B(CB, a final concentration of 1 μg/mL) into the AFM liquid chamber to inhibit actin filament polymerization. It is found that most signals disappear(1.2%), and the force value is similar as that before inhibition[Fig.4(B)]. The results indicate that RV particles enter cells mainly through the clathrin-mediated endocytosis, and our results are consistent with the previous report[12,30].

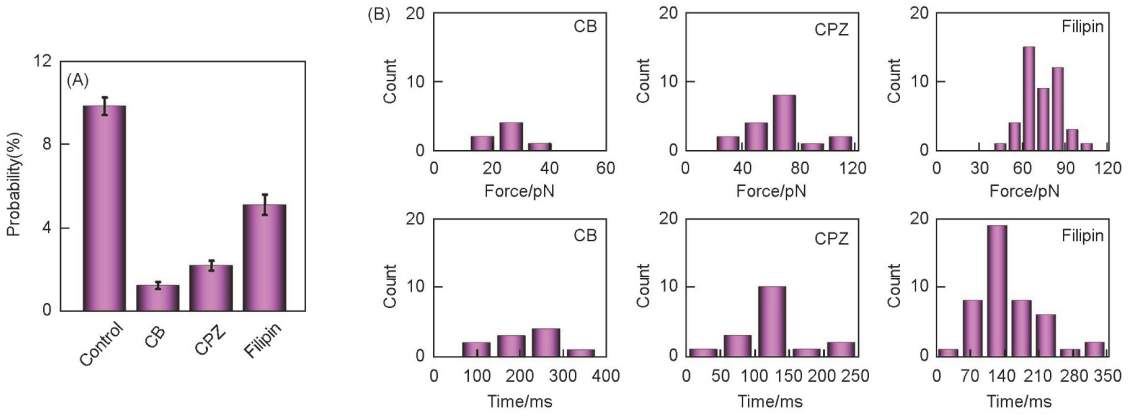

Fig.4 Blocking experiments

(A) Probability of force-time signals in force tracing curves before(control) and after inhibition with CB, CPZ and filipin; (B) force and duration distribution after blocking with CB, CPZ and filipin. The above results are the mean value of three independent experimental measurements, each of which was based on analyzing 1000 force tracing curves(the probability of the force-time signal is the number of typical force tracing curves divided by1000 randomly selected force tracing curves).

4 Conclusions

In conclusion, the dynamic mechanism of RV particles entering cell was discovered by using the high temporal-spatial resolution force tracing at the single-particle level. The dynamic process was monitored, and the parameters were detected. On the basis of experiment results, we propose a model that provides insight into the interactions between RV particles and cell membrane. This approach will be also useful for researching the interactions between cell membranes and other virus with various shapes and sizes.

Electronic Supplementary Material

Supplementary material is available in the online version of this article at http://dx.doi.org/10.1007/s40242-022-2069-y.

Acknowledgements

This work was supported by the Project of the Education Department of Jilin Province, China(No.JJKH20220666KJ), the Talent of Jilin Province Development Fund Project, China(No.2021Y004), and the National Natural Science Foundation of China(No.21773017).

Conflicts of Interest

The authors declare no conflicts of interest.

References

[1] Pringle C. R., *Arch. Virol.*, **1997**, *142*, 2321
[2] Fooks A. R., Cliquet F., Finke S., Freuling C., Hemachudha T., Mani R. S., Muller T., Nadin-Davis S., Picard-Meyer E., Wilde H., Banyard A. C., *Nat. Rev. Dis. Primers.*, **2017**, *3*, 17091
[3] Schnell M. J., McGettigan J. P., Wirblich C., Papaneri A., *Nat. Rev. Microbiol.*, **2010**, *8*, 51
[4] Fisher C. R., Streicker D. G., Schnell M. J., *Nat. Rev. Microbiol.*, **2018**, *16*, 241
[5] Nakagawa K., Kobayashi Y., Ito N., Suzuki Y., Okada K., Makino M., Goto H., Takahashi T., Sugiyama M., *J. Virol.*, **2017**, *91*, 20
[6] Khalifa M. E., Unterholzner L., Munir M., *Front. Cell. Infect. Mi.*, **2021**, *949*, 2235
[7] Yang F. L., Lin S., Ye F., Yang J., Qi J. X., Chen Z. J., Lin X., Wang J. C., Yue D., Cheng Y. W., Chen Z. M., Chen H., You Y., Zhang Z. L., Yang Y., Yang M., Sun H. L., Li Y. H., Cao Y., Yang S. Y., Wei Y. Q., Gao G. F., Lu G. W., *Cell Host Microbe.*, **2020**, *27*, 441
[8] Maginnis M. S., *J. Mol. Biol.*, **2018**, *430*, 2590
[9] Zhang Y., Wang Y. Y., Feng Y., Tu Z. Z., Lou Z. Y., Tu C. C., *Virol. Sin.*, **2020**, *35*, 143
[10] Lahaye X., Vidy A., Pomier C., Obiang L., Harper F., Gaudin Y., Blondel D., *J. Virol.*, **2009**, *83*, 7948
[11] Finke S., Brzozka K., Conzelmann K. K., *J. Virol.*, **2004**, *78*, 12333
[12] Xu H. J., Hao X., Wang S. W., Wang Z. Y., Cai M. J., Jiang J. G., Qin Q. W., Zhang M. L., Wang H. D., *Sci. Rep.*, **2015**, *5*, 1
[13] Zhang Q., Tian F. L., Wang F., Guo Z. Y., Cai M. J., Xu H. J., Wang H. D., Yang G. C., Shi X. H., Shan Y. P., Cui Z. Q., *ACS Nano*, **2020**, *14*, 7046
[14] Zhang Q. R., Li S. Y., Yang Y., Shan Y., Wang H. D., *Biophysics Rep.*, **2021**, *7*, 384
[15] Xue M., Heldt C. L., *Bio.Techniques.*, **2020**, *69*, 5
[16] Stroh C., Wang H., Bash R., Ashcroft B., Nelson J., Gruber H., Lohr D., Lindsay S. M., Hinterdorfer P., *Proceedings of the National Academy of Sciences*, **2004**, *101*, 12503
[17] Shan Y., Ma S., Nie L., Shang X., Hao X., Tang Z., Wang H., *Chemical Communications*, **2011**, *47*, 8091
[18] Zhao W. D., Tian Y. M., Cai M. J., Wang F., Wu J. Z., Gao J., Liu S. H., Jiang J. G., Jiang S. B., Wang H. D., *PLoS One*, **2014**, *9*, e91595
[19] Yang K., Ma Y. Q., *Nat. Nanotechnol*, **2010**, *5*, 579
[20] Kienberger F., Pastushenko V. P., Kada G., Gruber H. J., Riener C., Schindler H., Hinterdorfer P., *Single. Mol.*, **2000**, *1*, 123
[21] Mercer J., Schelhaas M., Helenius A., *Annu. Rev. Biochem.*, **2010**, *79*, 803
[22] Sun X. W., Zheng W. Y., Hua R., Liu Y. J., Yoshida S., *Blood & Genomics*, **2021**, *5*, 1
[23] Bayati A., Kumar R., Francis V., McPherson P. S., *J. Biol. Chem.*, **2021**, *296*, 100306
[24] Glebov O. O., *FEBS. J.*, **2020**, *287*, 3364
[25] Cossart P., Helenius A., *CSH. Perspect. Biol.*, **2014**, *6*, a016972
[26] Zhang F. X., Guo H., Zhang J., Chen Q. X., Fang Q., *Virology.*, **2017**, *513*, 195
[27] Swanson J. A., King J. S., *Philos. T. R. Soc. B*, **2019**, *374*, 20180146
[28] Wei X., She G., Wu T., Xue C., Cao Y., *Vet. Res.*, **2020**, *51*, 10
[29] Pan W., Nie H., Wang H. M., He H. B., *Viruses*, **2021**, *13*, 1035
[30] Piccinotti S., Kirchhausen T., Whelan S. P. J., *J. Virol.*, **2013**, *87*, 11637